scientific reports

OPEN

Efficacy of robot arm-assisted endoscopic submucosal dissection in live porcine stomach (with video)

Joonhwan Kim[1], Dong-Ho Lee[1], Dong-Soo Kwon[1,2], Ki Cheol Park[3], Hae Joung Sul[4], Minho Hwang[5] & Seung-Woo Lee[6]✉

Endoscopic submucosal dissection (ESD) is technically challenging and requires a high level of skill. However, there is no effective method of exposing the submucosal plane during dissection. In this study, the efficacy of robot arm-assisted tissue traction for gastric ESD was evaluated using an in vivo porcine model. The stomach of each pig was divided into eight locations. In the conventional ESD (C-ESD) group, one ESD was performed at each location (N = 8). In the robot arm-assisted ESD (R-ESD) group, two ESDs were performed at each location (N = 16). The primary endpoint was the submucosal dissection speed (mm^2/s). The robot arm could apply tissue traction in the desired direction and successfully expose the submucosal plane during submucosal dissection in all lesion locations. The submucosal dissection speed was significantly faster in the R-ESD group than in the C-ESD group ($p = 0.005$). The blind dissection rate was significantly lower in the R-ESD group ($P = 0.000$). The robotic arm-assisted traction in ESD enabled a significant improvement in submucosal dissection speed, blind dissection rate which suggests the potential for making ESD easier and enhancing procedural efficiency and safety.

Keywords Endoscopic mucosal resection, Stomach neoplasm, Robotic surgical procedure, Traction, Animal experimentation

The use of endoscopic submucosal dissection (ESD) as a radical treatment for early-stage gastrointestinal cancer has been increasing with the development of endoscopic therapeutic techniques and instrumentation. However, ESD is technically challenging and requires a high level of skill. Furthermore, there is no effective method of exposing the submucosal plane during dissection (Fig. 1a). Dissection performed under the unclear visibility of the submucosal plane not only increases the difficulty of the procedure but also increases the risk of complications such as unexpected perforation or bleeding[1,2].

To solve this problem, several tissue traction methods, such as clip-with-line[3,4], S–O clips[5,6], and magnetic anchors[7,8] have been proposed to lift the mucosal flap during dissection. Additionally, traction methods using externally mounted forceps[9,10] and an articulating robot arm[11], which are attached to the exterior of an endoscope, have been devised. However, conventional methods have limitations, such as difficulty in adjusting the grasping position and controlling the traction direction and tension, thus limiting their applicability and efficacy. In the author's previous work, an articulating robot arm that can be attached to a commercial endoscope was proposed. The robotic arm facilitates tissue traction in various directions and tension, and its feasibility has been validated using an ex vivo porcine gastric model[12].

In this study, the efficacy of robot-assisted tissue traction for gastric ESD was evaluated using an in vivo porcine model. As far as the author's knowledge, this is the first study that examined the efficacy of the robot arm-assisted ESD throughout the various parts of the stomach including a location adjacent to a gastric cardia, and investigated the efficacy according to the lesion location and size.

[1]R&D Center, Roen Surgical, Inc., Daejeon, South Korea. [2]Department of Mechanical Engineering, Korea Advanced Institute of Science and Technology, Daejeon, South Korea. [3]Clinical Research Institute, Daejeon St. Mary's Hospital, The Catholic University of Korea, Daejeon, South Korea. [4]Department of Pathology, College of Medicine, The Catholic University of Korea, Seoul, South Korea. [5]Department of Robotics and Mechatronics Engineering, Daegu Gyeongbuk Institute of Science and Technology, Daegu, South Korea. [6]Division of Gastroenterology, Department of Internal Medicine, College of Medicine, The Catholic University of Korea, Seoul, Korea. ✉email: leeseungw0@catholic.ac.kr

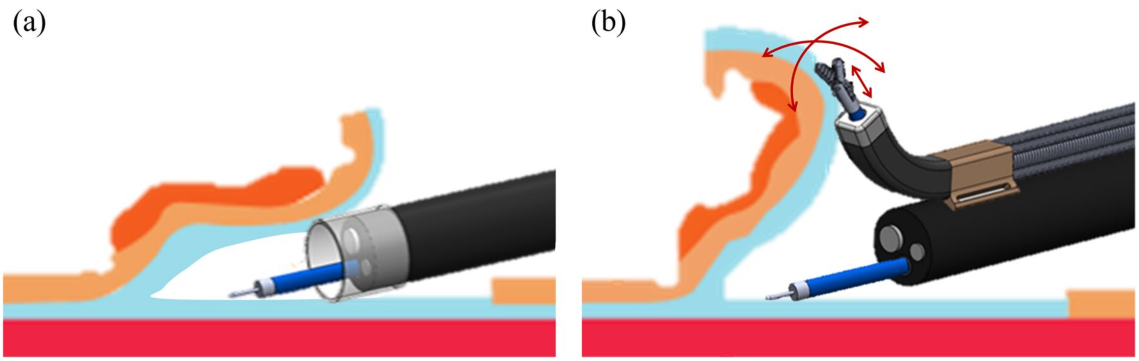

Figure 1. (**a**) Conventional endoscopic submucosal dissection (ESD). (**b**) Robot arm-assisted ESD.

Methods

Endoscope-attachable robot arm for tissue traction

The proposed robotic arm can grasp a mucosal flap and manipulate it in the desired direction to expose the submucosal plane and apply proper tissue tension during dissection (Fig. 1b). The robot arm can be bent up, down, left, and right up to 100 degrees. The thickness of the robot arm is 5-mm × 5-mm and the total length of the articulated part is 25-mm (Fig. 2a). It contains a 2.8-mm working channel for introducing commercial endoscopic instruments such as forceps for tissue grasping (Fig. 2a). The instruments can be inserted and withdrawn through the channel. The bending of the robot arm can be controlled using a thumb stick controller. The details of the system configuration and specifications have been described previously[12]. The robot arm can be tied to the exterior of the distal end of a commercial gastrointestinal endoscope using surgical tape. In a scenario involving robot arm-assisted ESD, an endoscopist manipulates an endoscope and the assistant operates the robot arm and commercial endoscopic forceps (Fig. 2b).

Experimental setting

Live minipigs (*Sus scrofa domestica*) fasted for 48 h. Each pig weighed approximately 50 kg. General anesthesia was administered with an injection of Zoletil 50 (5 mg/kg; Virbac, France) and xylazine (2.5 mg/kg; Rompun®; Bayer AG, Germany). The pigs were intubated, and anesthesia was maintained with 1% to 2% isoflurane added to oxygen gas using a ventilator. The heart rate and oxygen saturation were monitored throughout the experiment. One pig was used for each session, and a total of four sessions were performed. No inclusion and exclusion criteria were set.

The number of experiments was determined using previous ex vivo experimental data[12]. It was assumed that there was a difference of 74.8 mm^2/min in the submucosal dissection speed between conventional ESD (C-ESD) and robot arm-assisted ESD (R-ESD). The procedure was performed using a 1:2 ratio for the C-ESD and R-ESD groups. The required number of experiments was 24 for a 5% level of significance and power of 80%. Therefore, the C-ESD procedure was performed eight times and the R-ESD procedure was performed 16 times.

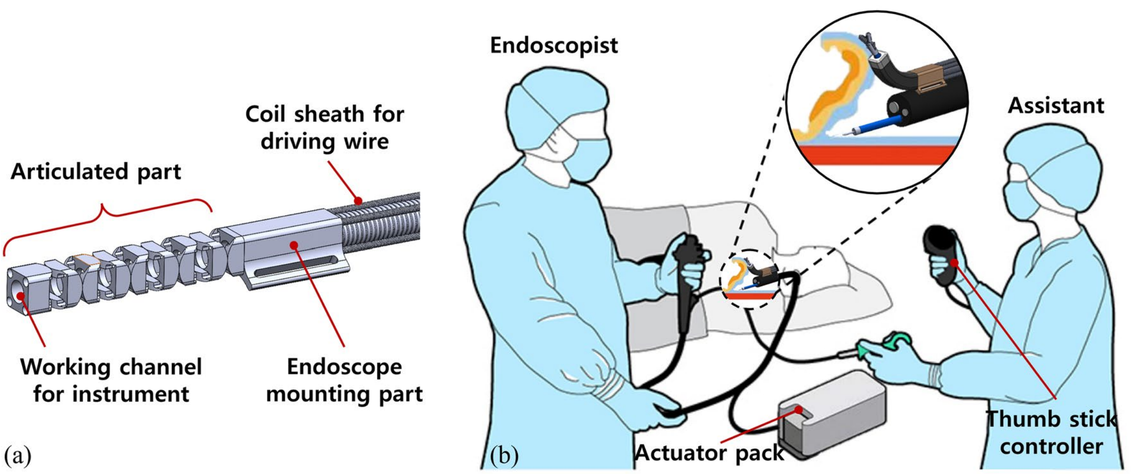

Figure 2. (**a**) Configuration of the robot arm. (**b**) Conceptual diagram of the use of robot arm assistance during endoscopic procedures.

ESD procedure

The stomach of each pig was divided into eight locations: upper anterior wall; upper posterior wall; upper lesser curvature; upper greater curvature; lower anterior wall; lower posterior wall; lower lesser curvature; and lower greater curvature. The upper and lower parts were divided based on the gastric angle. ESD was performed at each location using upper gastrointestinal endoscopy (GIF Q260J, GIF-2TQ260M; Olympus Inc., Tokyo, Japan). In the C-ESD group, a single ESD was performed at each location. In the R-ESD group, two ESDs were performed at each location.

During the ESD procedure (Fig. 3), a pseudolesion with a diameter of approximately 2 to 3 cm was marked using a hook knife (KD-620 LR; Olympus, Tokyo, Japan) at each site. A mixture of normal saline and indigo carmine was injected into the submucosal layer. Mucosal incision and submucosal dissection were performed using a hook knife and an IT knife (KD-611L; Olympus, Tokyo, Japan). In the R-ESD group, the endoscope was withdrawn from the body after the completion of the mucosal incision to attach the robot arm to the endoscope. The robot arm was tied along the axis of the endoscope; the attached location differed depending on the location of the lesion. Hemostasis was performed using a coagrasper (FD-410LR; Olympus, Tokyo, Japan) during the procedure in cases of active bleeding that interfered with the procedure. After completion of submucosal dissection, the lesion was inspected for complete resection, bleeding, and perforation. Then, the specimens were extracted and subjected to histological examination. The specimens were sectioned at 4 mm, and they were embedded in paraffin and stained with hematoxylin and eosin. In the C-ESD group, a transparent cap was attached to the tip of the endoscope throughout the procedure. The order of the procedure was determined by drawing lots on a piece of paper indicating the group and lesion locations. All ESDs were performed by an expert endoscopist who had more than 10 years of experience of performing gastrointestinal ESD and experience with more than 1000 cases of gastric ESD. The mucosal incision and submucosal dissection were performed using an electrosurgical system (ERBE VIO 300D; Erbe, USA) with the following settings: Endocut Q, effect 2, cut duration 3, and cut interval 4. Video 1 demonstrates the robot-arm assisted ESD procedure at the lower part greater curvature.

Outcomes and their definitions

Various outcomes related to the procedure and histological analysis were compared between the C-ESD and R-ESD groups. The primary endpoint was the submucosal dissection speed (mm^2/s). Secondary endpoints related to the procedure were the resected specimen area (mm^2), total procedure time (s), marking time (s), mucosal incision time (s), submucosal dissection time (s), blind dissection rate (%), en bloc resection rate (%), complete resection rate (%), injection volume (ml), number of instrument replacements, and complications such as bleeding and perforation. In the R-ESD group, the robot arm application time (s) and tissue damage during endoscope insertion were also evaluated. Secondary endpoints related to the histologic analysis were total thickness (μm), submucosal thickness (μm), vertical submucosal thermal damage (μm), and horizontal submucosal thermal damage (μm).

The marking time, injection time, mucosal incision time, and submucosal dissection time were defined as the time from the start of the procedure to the end of the procedure. The total procedure time was defined as the time from marking to specimen withdrawal. The resected specimen area was measured using image processing software (ImageJ; National Institutes of Health, Bethesda, MD, USA) when it was stretched out. Dissection speed was defined by dividing the specimen size by the dissection time. The blind dissection rate was defined as the

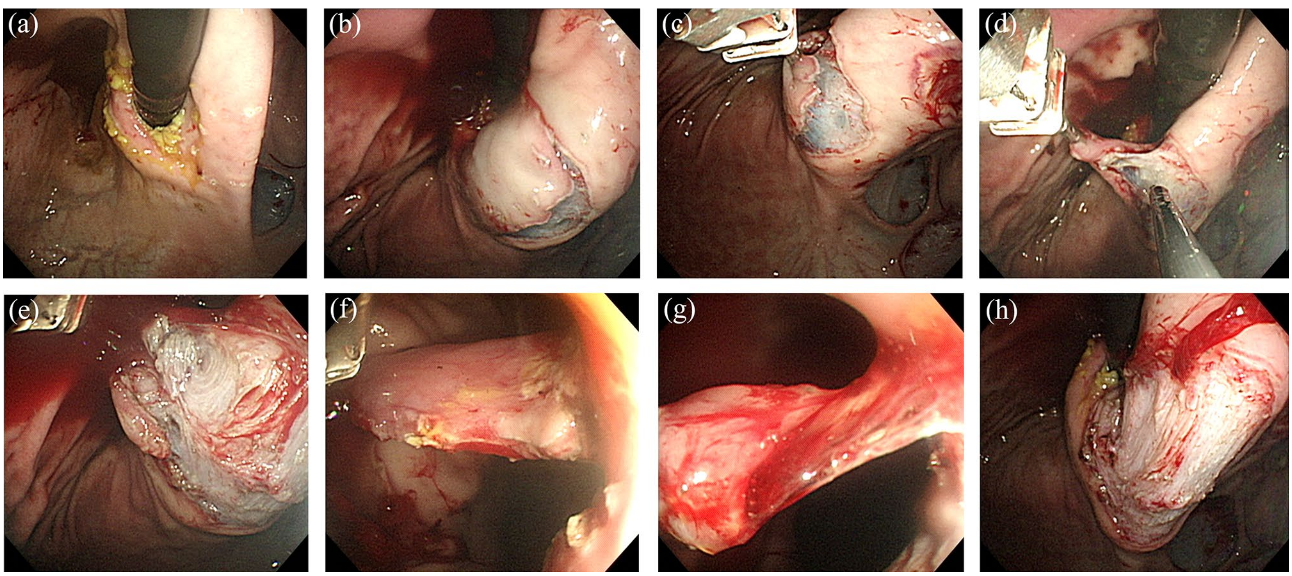

Figure 3. Robot arm-assisted endoscopic submucosal dissection (ESD). (**a**) Marking at the lesser curvature side of the upper body. (**b**) Completion of the mucosal incision. (**c**) Initial stage of traction by the robot arm. (**d**) Intermediate stage of traction. (**e**) Late stage of traction. (**f**) Traction during the forward approach. (**g**) Few submucosal tissues remained. (**h**) Completion of ESD.

percentage of submucosal dissection time during which the submucosal dissection plane was not exposed. The en bloc resection rate was defined as the percentage of one-piece resections. The complete resection rate was defined as the percentage of complete excision of the marked area. To determine the thickness of the resected specimen, the average of the two thickest regions on each slide was examined. Submucosal thermal damage was defined as the depth from the superficial portion of the resected specimen that presented fibrinonecrotic changes and infiltration of inflammatory cells. The measurement was performed in the same way as described previously[12]. The robot arm application time was defined as the total time required to withdraw the endoscope after incision, attach the robot arm, and insert the endoscope into the lesion again.

Statistical analysis

Continuous variables are expressed as the mean ± standard deviation and the median and interquartile range based on normality using the Shapiro–Wilk test. Categorical variables were expressed as percentiles. Depending on normality, the differences in continuous variables were analyzed using the independent t-test or Mann–Whitney U test. Differences in categorical variables were analyzed using Fisher's exact test. For all cases, statistical significance was set at $p < 0.05$. All statistical analyses were performed using IBM SPSS Statistics (version 26.0; SPSS Inc., Chicago, IL, USA).

Ethics

All methods were performed in accordance with the relevant guidelines and regulations. The study was designed and carried out in compliance with the ARRIVE guidelines on animal research. This study was approved by the Institutional Animal Care and Use Committee of KNOTUS (KNOTUS IACUC 20-KE-233).

Results

All ESDs were successfully completed in both groups. In the R-ESD group, the robotic arm can be smoothly applied to the workflow of the routine ESD procedure. No critical problem in the coordination between the endoscopist and the assistant was observed during the use of the robot arm. The robot arm worked well without system failures in 16 cases. The robot arm could apply tissue traction in the desired direction and successfully expose the submucosal plane during submucosal dissection in all lesion locations (Fig. 4). No mucosal damage was visible in the pharyngeal or esophageal inlet area after the insertion of the endoscope with the robot arm attached.

The overall outcomes are presented in Table 1 and Fig. 5. Regarding the primary outcome, submucosal dissection speed was significantly faster in the R-ESD group than in the C-ESD group ($p = 0.005$). Regarding the secondary outcomes related to the procedure, the resected specimen area and total procedure time were comparable between groups ($p = 0.787$ and $p = 0.585$, respectively). The marking and mucosal incision times were not significantly different between groups ($p = 0.312$ and $p = 0.127$, respectively). The submucosal dissection time decreased by 40.8% in the R-ESD group, although the difference was not significant ($p = 0.109$). The blind dissection rate was significantly lower in the R-ESD group ($P = 0.000$). En bloc and complete resection were performed in both groups. The injection volume and number of instrument replacements were significantly lower in the R-ESD group ($p = 0.008$ and $p = 0.000$, respectively). No perforation occurred in the R-ESD group and one perforation occurred in the C-ESD group (not significantly different; $p = 0.333$). Two cases of bleeding occurred in

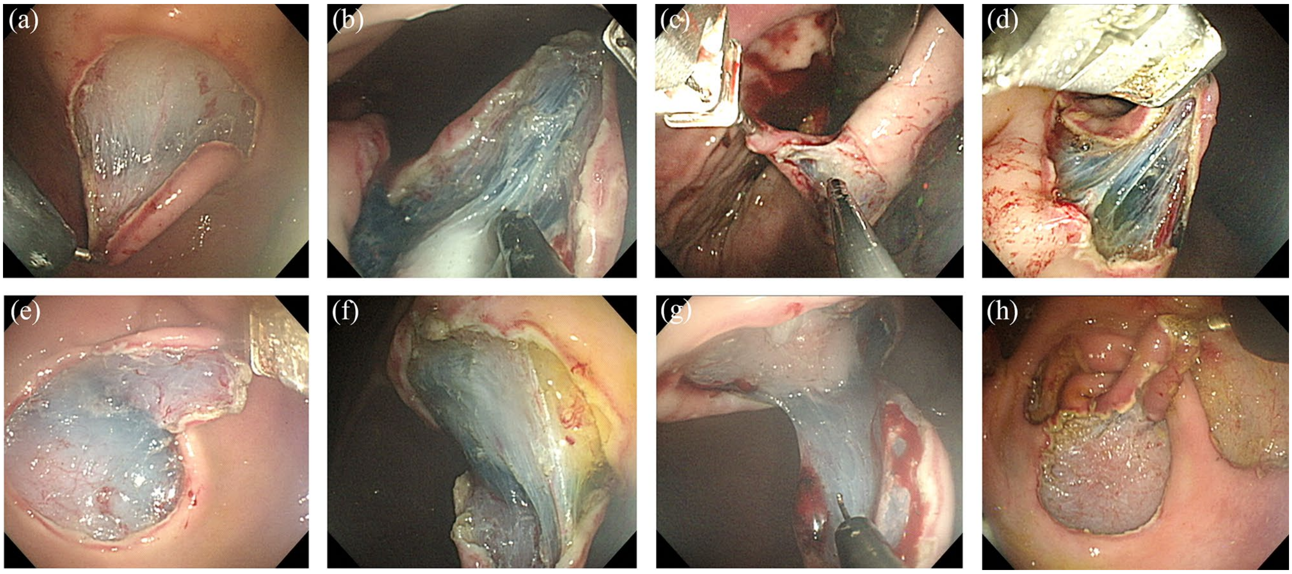

Figure 4. Tissue traction and submucosal plane exposure using the robot arm at each lesion location. (**a**) Upper anterior wall. (**b**) Upper posterior wall. (**c**) Upper lesser curvature. (**d**) Upper greater curvature. (**e**) Lower anterior wall. (**f**) Lower posterior wall. (**g**) Lower lesser curvature; and (**h**) Lower greater curvature.

Variables	C-ESD (N = 8)	R-ESD (N = 16)	p-value
Resected specimen area (mm^2)	1363.0 (1268.1–1656.4)	1280.4 (1180.2–1704.1)	0.787
Total procedure time (s)	1203.8 ± 585.2	1081.4 ± 238.6	0.585
Marking time (s)	49.1 ± 32.2	36.5 ± 9.8	0.312
Mucosal incision time (s)	172.5 ± 71.0	227.8 ± 84.6	0.127
Robot arm application time (s)	–	210.6 ± 61.7	NA
Submucosal dissection time (s)	845.1 ± 518.3	500.1 ± 241.9	0.109
Submucosal dissection speed (mm^2/s)	2.2 ± 0.9	3.9 ± 1.8	0.005
Blind dissection rate (%)	15.4 (10.9–22.3)	0.0 (0.0–0.6)	0.000
Injection volume (mL)	22.6 ± 6.8	15.2 ± 5.3	0.008
Instrument changes (no.)	8.0 ± 2.6	2.8 ± 1.3	0.000
En bloc resection, n (%)	8 (100.0)	16 (100.0)	NA
Complete resection, n (%)	8 (100.0)	16 (100.0)	NA
Perforation, n (%)	1 (12.5)	0 (0.0)	0.333
Bleeding, n (%)	0 (0.0)	2 (12.5)	0.536
Specimen total thickness (μm)	1253.4 ± 342.8	1218.5 ± 370.7	0.826
Specimen submucosal thickness (μm)	409.4 (366.7–468.8)	386.0 (287.5–562.5)	0.697
Submucosal damage (vertical) (μm)	114.3 ± 53.7	88.0 ± 35.1	0.161
Submucosal damage (lateral) (μm)	159.3 ± 91.3	119.3 ± 41.5	0.150

Table 1. Outcomes of the C-ESD group and R-ESD group. C-ESD, conventional endoscopic submucosal dissection; ESD, endoscopic submucosal dissection; NA, not applicable; R-ESD, robot arm-assisted endoscopic submucosal dissection. Values are presented as the mean ± standard deviation for normally distributed data and as a median and interquartile range for non-normally distributed data.

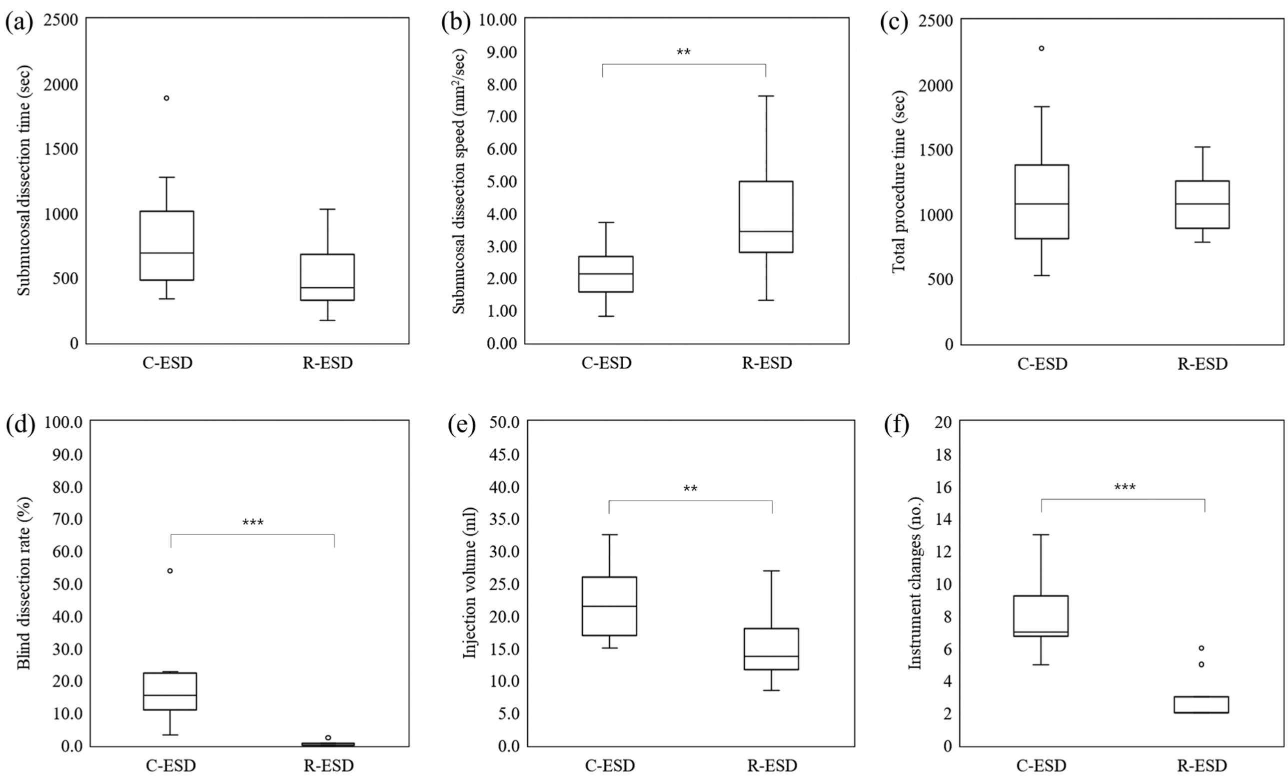

Figure 5. Outcomes of the C-ESD group and R-ESD group. (**a**) Submucosal dissection time. (**b**) Submucosal dissection speed. (**c**) Total procedure time. (**d**) Blind dissection rate. (**e**) Injection volume. (**f**) Instrument changes. The symbol ** and *** represents $p < 0.01$ and $p < 0.001$, respectively. The symbol ○ represents outliers.

the R-ESD group and no bleeding occurred in the C-ESD group (not significantly different; p = 0.536). Regarding the secondary outcomes related to the histologic analysis, the total thickness and submucosal thickness were not significantly different between groups (p = 0.826 and p = 0.697, respectively). The submucosal damage in the vertical direction and that in the horizontal direction decreased by 23.0% and 25.2%, respectively, in the R-ESD group; however, they were not significantly different (p = 0.161 and p = 0.150, respectively). The subanalysis outcomes are described in Tables 2 and 3, and Figs. 6 and 7. Regarding the lesion location, the improvements in the total procedure time, dissection time, and dissection speed were more prominent in the upper stomach than in the lower stomach although there is no statistical difference (Table 2 and Fig. 6). Due to the limited sample size, no statistical significance or clear trend was confirmed based on the location such as lesser curvature/greater curvature and anterior wall/posterior wall (Supplementary tables and figures). Overall, there was a tendency for increased dissection speed and decreased dissection time in the R-ESD group across all locations. Regarding the resected specimen area, the two groups were divided based on the median resection area. The improvements in the total procedure time, dissection time, and dissection speed were more prominent in the larger specimen area group than in the smaller specimen area group (Table 3 and Fig. 7).

Lesion location	Variables	C-ESD (N = 4)	R-ESD (N = 8)	p-value
Upper stomach	Total procedure time (s)	1529.5 (1226.8–1941.8)	1272.0 (1066.5–1350.8)	0.368
	Dissection time (s)	1104.0 (884.3–1431.3)	706.5 (503.5–795.8)	0.073
	Dissection speed (mm^2/s)	1.5 (1.3–1.9)	3.3 (2.1–5.2)	0.109
Lower stomach	Total procedure time (s)	804.0 (725.3–847.3)	867.5 (786.8–1078.5)	0.461
	Dissection time (s)	472.0 (422.3–528.5)	329.0 (275.0–416.0)	0.073
	Dissection speed (mm^2/s)	2.4 (2.2–2.9)	3.4 (3.0–4.7)	0.073

Table 2. Total procedure time, dissection time, and dissection speed based on the lesion location. C-ESD, conventional endoscopic submucosal dissection; R-ESD, robot arm-assisted endoscopic submucosal dissection. Values are presented as the median and interquartile range.

Specimen area	Variables	C-ESD (N = 4)	R-ESD (N = 8)	p-value
Smaller specimen	Specimen area (mm^2)	1261.7 (1181.9–1288.8)	1159.0 (976.0–1218.1)	0.214
	Total procedure time (s)	804.0 (725.3–847.3)	921.5 (812.8–1114.8)	0.283
	Dissection time (s)	472.0 (422.3–528.5)	416.5 (281.0–434.0)	0.283
	Dissection speed (mm^2/s)	2.4 (2.2–2.9)	2.9 (2.6–3.7)	0.368
Larger specimen	Specimen area (mm^2)	1786.3 (1493.4–2067.5)	1776.0 (1552.3–3046.6)	0.570
	Total procedure time (s)	1529.5 (1226.8–1941.8)	1164.5 (1059.8–1306.8)	0.214
	Dissection time (s)	1104.0 (884.3–1431.3)	596.5 (362.3–531.0)	0.048
	Dissection speed (mm^2/s)	1.5 (1.3–1.9)	4.2 (3.4–5.7)	0.016

Table 3. Total procedure time, dissection time, and dissection speed based on the resected specimen area. Values are presented as the median and interquartile range.

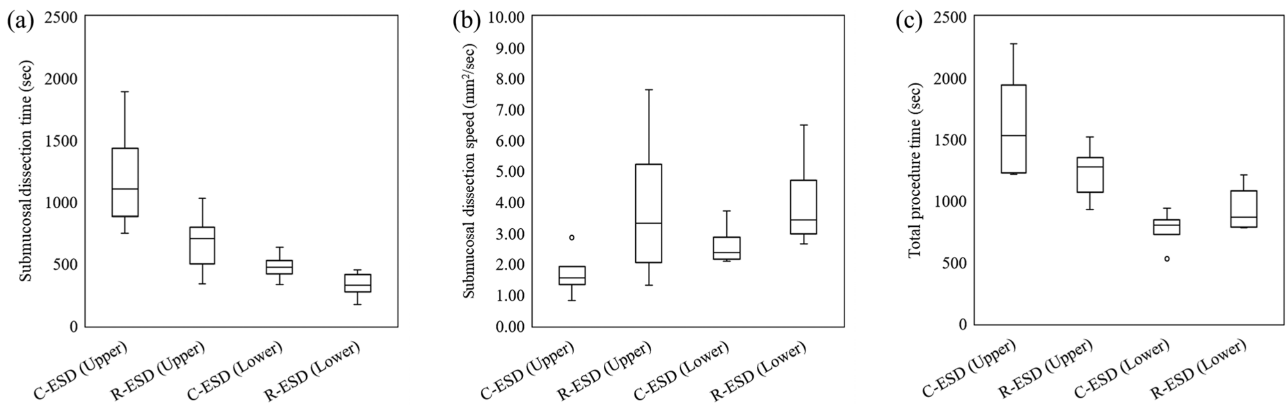

Figure 6. Outcomes of the C-ESD group and R-ESD group based on the lesion location. (**a**) Submucosal dissection time. (**b**) Submucosal dissection speed. (**c**) Total procedure time. The symbol ○ represents outliers.

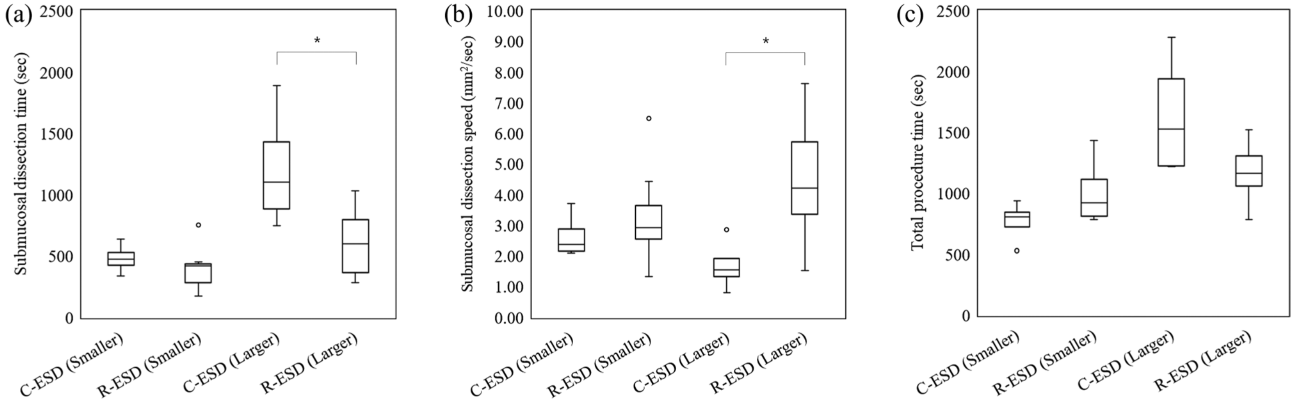

Figure 7. Outcomes of the C-ESD group and R-ESD group based on the resected specimen area. (**a**) Submucosal dissection time. (**b**) Submucosal dissection speed. (**c**) Total procedure time. The symbol * represents $p < 0.05$. The symbol ○ represents outliers.

Discussions

The proposed robotic arm successfully facilitated tissue traction in an in vivo swine stomach at various lesion locations. In particular, dissection using traction was successfully performed even in lesions adjacent to gastric cardia, which is a difficult area to perform. Pigs are commonly used as a translational model of gastrointestinal function, being of similar size and having comparable gastrointestinal anatomy and physiology to humans[13]. In addition, the live porcine model simulates the influence of breath and heartbeat and provides the environment to deal with adverse events such as perforation and bleeding[14]. Therefore, the experimental results observed in such environments demonstrated the feasibility of applying the robot arm in clinical practices.

Ease of control of both traction direction and force, and ease of re-grasping of the tissue with the low risk of tissue damage at the grasping site in various gastric lesion locations is the biggest advantage of the proposed robot arm-assisted traction compared to the conventional traction methods. The method using the clip-with-line is simple and low cost, however, the traction direction is limited to the direction in which the line is pulled, which limits the indication. In addition, too strong pulling can cause the slip-off of the clip from the lesion. The method using the S–O clip is effective and can control the traction direction by the selection of the anchoring location. It can also vary the traction force by inflating or deflating the organ. However, the traction direction is difficult to be adaptively changed during the dissection, and the control of the traction force might not be delicate. In addition, the spring can interfere with the endoscope in case of a retroflexion approach, which may limit its usage[5]. The method using the magnetic anchor is promising and can provide traction in various directions and forces although it requires an additional specific external magnet[7]. There might be a concern that the anchoring stability can be affected by the lesion location, and the patient's obesity, therefore, its usage and effectiveness need to be further investigated. It is important to select a proper clipping site in all clip-based methods since inappropriate clipping can interrupt procedures and adjustment of the clipping site is difficult. In addition, there is a risk of normal tissue damage at the clipping site. The method using externally mounted forceps can control the traction force and allow easy change of traction point. However, the motion of the forceps is synchronized with the endoscope and has a limited independent motion from the endoscope. This limits the optimal control of the traction direction during the dissection. The advantage of the robot arm traction will contribute to securing better visibility of the submucosal plane and tissue tension for efficient and safe dissection compared to conventional traction methods although this should be further investigated. The attached video demonstrates the adjustment of the traction direction and force during the dissection. In general, the robot arm traction can be effective in areas such as greater curvature of the gastric body and lesser curvature of the gastric antrum where it is difficult to utilize the gravitational traction. In addition, from our experiences, we found that it can be effective in areas such as gastric fundus where traction from multiple directions is required. In particular, the robot arm-assisted traction enabled a forward approach in a lesion location such as in the gastric body or gastric cardia where the endoscope usually approaches in a retroflexed posture in the conventional ESD. This allows an endoscopist to perform ESD with more ease and less fatigue of the hand. In addition, if the robot arm is improved for further miniaturization, robot arm traction can be useful for lesions in the duodenum or large intestine that are difficult to apply clip-based traction. Although the control of the robot arm requires a certain amount of training, in our study, the assistant could adapt to the control of the robot arm with little experience because the motion of the robot arm is directly synchronized to the motion of the thumb stick controller and the shape of the robot arm is visually displayed through the robot arm software.

The submucosal dissection speed significantly increased in the R-ESD group. This result was mainly attributed to the superior exposure of the submucosal plane and the tissue tension achieved by tissue traction. Moreover, it was noted that robot arm-assisted traction was more effective for lesions located in the upper stomach and larger lesions. During conventional ESD, the upper stomach is more technically challenging than that in the mid or lower stomach because retroflexion is more frequently required, and the operator is hard to allow the knife to encroach the submucosal layer beneath the tumor and to control the direction and depth while adhering to the dissection plan[15]. However, with the help of the robot arm, it was easier to expose the submucosal plane and perform submucosal dissection. Additionally, during conventional ESD, as the lesion became larger, the loosened flap was more out of control and interfered with the movement of the endoscope. The operator was required to place the flap aside and perform dissection simultaneously, resulting in considerable physical and mental burdens[12]. When these situations occur, the tissue traction provided by the robotic arm alleviates these difficulties. Since the robot arm is attached to the endoscope, we faced situations where the direction and force of the traction were influenced by the motion of the endoscope during the cutting. However, in most cases with lesions sized between 2–3 cm, we were able to achieve the desired traction by adjusting the magnitude and direction of the bending of the robot arm. The motion of the robot arm was not sufficient to apply adequate traction in several cases involving larger lesions or lesions that required significant bending of the endoscope. In such cases, we were able to provide effective traction by re-grasping the appropriate site of the flap or attaching the robot arm at a different position of the endoscope.

Instrument replacement was significantly reduced in the R-ESD group. This was mainly attributed to the decreased injection during submucosal dissection. In the C-ESD group, multiple injections were required for effective dissection, whereas less injection was required in the R-ESD group because of superior exposure of the submucosal plane. For the same reason, the injection volume significantly decreased in the R-ESD group. Because the large volume of injection fluid is thought to be a factor associated with gastric ischemia[16] and myocardial infarction[17], the robot arm-assisted traction may contribute to reducing the risk of injection-related complications as well. In this study, we compared R-ESD with C-ESD using knives without injection capability and normal saline as injection fluid. Recent publications also used normal saline as an injection fluid, and it has been used as a comparison between conventional and robotic-assisted ESD[11,18,19]. However, the use of knives with injection capability or long-lasting injection fluid could potentially reduce the number of instrument replacements and injection volumes in the conventional ESD.

Excellent exposure of the submucosal plane also resulted in a significant decrease in the blind dissection rate of the R-ESD group. In particular, traction can be effective for alleviating the blind resection in some cases, such as when the initial stage of the submucosal dissection involved little or no flap to be elevated, the location of the endoscope made it difficult to approach the submucosal plane, and when the location had no gravitational traction. Blind dissection should be avoided to minimize the risks of perforation and bleeding[2]. In this context, the absence of perforation in the R-ESD group may be attributed to the significantly improved blind dissection rate. During C-ESD, the elevation of the mucosal flap and visualization of the submucosal dissection plane are the most difficult skills for novices[11]. Because operator experience is inversely related to the occurrence of perforations[20], it can be inferred that tissue traction would be more beneficial for less experienced endoscopists. Recent publications imply the benefit of robot arm-assisted traction for novice endoscopists[11,21]. This should be investigated further.

In contrast, although the submucosal plane was sufficiently exposed during dissection in the R-ESD group, two cases of bleeding occurred. This may be attributable to the increased dissection speed. The increased dissection speed may lead to a shallower coagulation effect and, thus, higher rates of intraoperative bleeding[22]. The reduced submucosal thermal damage in the R-ESD group may be explained by the same reason. In addition, the presence of a distance between the endoscope and the dissection tissue plane may have contributed to missing the detection of vessels requiring precoagulation. An optimization of the design and mounting position of the robot arm could shorten the distance. Adding a translational movement to the robot arm could be promising to optimize the viewing distance. Furthermore, the indigo carmine-mixed fluid injected into the submucosal layer may have stained vessels bluish, making them less visible. We believe that reducing the concentration of indigo carmine during the injection may help prevent bleeding. In case of bleeding, since the robot arm exposes the dissected surface, it may be beneficial in locating bleeding.

Although the robotic arm-assisted traction improved the dissection efficiency in all cases, the total procedure time was increased in some cases, such as when the lesion was located in the lower stomach and when the lesion was small. This is mainly because of the additional time required for the robot arm application. In addition to the time required for robot arm attachment, more time was required to carefully insert the endoscope with the protruding robot arm into the pharyngolarynx and esophagus.

Several similar attachable robot arms have been proposed for tissue traction during ESD[10,11,23]. The results are promising and demonstrate the feasibility of robot arm-assisted traction for improving procedural efficiency and safety. Moreover, recent advancements in robot technology have led to the emergence of robotic flexible endoscope systems that independently move two articulating robot arms from an endoscope[24–29]. However, these advanced systems have limitations, such as a large footprint, long setup time, and high costs, that require further refinement for successful clinical application. In addition, in most studies, the feasibility of robot arm assistance has only been verified for the limited lesion locations while ESD was attempted in various parts of the stomach including the retroflexion of the endoscope in this study.

Despite the several clinical benefits offered by the proposed robot arm, a few limitations of the robot arm were identified. First, the protrusion of the robot arm during endoscope insertion should be improved for safer and smoother endoscope insertion. The use of an overtube during the endoscope insertion can be promising. In addition, design modification to be capable of retraction of the robot arm through the working channel attached to the exterior of the endoscope during the endoscope insertion can be effective. Second, the robot arm should be further miniaturized for the application to narrower lumens such as esophagus and colon. A next-generation robot arm having a smaller diameter was developed at the point of the manuscript writing and the feasibility of esophageal ESD was evaluated.

This study has some limitations, such as the small sample size and limited user participation. In particular, the efficacy of the proposed method may differ by the ESD proficiency of the endoscopist. Therefore, further investigation with a larger sample size and more participants including the inexperienced endoscopist will be conducted. This first in-vivo study focused on the comparison with the conventional ESD to initially validate the feasibility and efficacy of the robot arm-assisted ESD. Further studies will include the comparison with currently available tissue traction methods such as Clip-with-line or S–O clip to clarify the benefit of the robot arm traction. In addition, we will focus on safety validation to identify the potential complications associated with the use of a robot arm. This will include the investigation of proper electrocoagulation settings to reduce the shallow coagulation effect during the dissection under robot arm traction and a detailed inspection of tissue damage caused by the contact of the robot arm during insertion and tissue manipulation. In addition, the porcine model provides similar characteristics to humans, however, it may not fully replicate the human cases. The translation of these findings to clinical practice in humans will be further investigated. Although there are several limitations and further studies are required for the comprehensive investigation of the benefit of robot arm-assisted ESD, we believe that the results demonstrated the potential for improving efficiency and safety in the robot arm-assisted traction for gastric ESD even for the expert endoscopist.

In conclusion, robot arm-assisted traction is feasible in vivo. It was proven that superior exposure of the submucosal plane during dissection enabled a significant improvement in the submucosal dissection speed, blind dissection rate, injection volume, and number of instrument replacements. Improvements in these outcomes suggest the potential for making ESD easier and enhancing procedural efficiency and safety with this robot arm.

Data availability

The final datasets analyzed during the current study are available from the supplementary materials.

Received: 14 November 2023; Accepted: 30 May 2024
Published online: 29 July 2024

References

1. Hatta, W. *et al.* Recent approach for preventing complications in upper gastrointestinal endoscopic submucosal dissection. *DEN Open* **2**, e60 (2022).
2. Oyama, T. Esophageal ESD: Technique and prevention of complications. *Gastrointest. Endosc. Clin. N. Am.* **24**, 201–212 (2014).
3. Yoshida, M. *et al.* Efficacy of endoscopic submucosal dissection with dental floss clip traction for gastric epithelial neoplasia: A pilot study (with video). *Surg. Endosc.* **30**, 3100–3106 (2016).
4. Suzuki, S. *et al.* Usefulness of a traction method using dental floss and a hemoclip for gastric endoscopic submucosal dissection: A propensity score matching analysis (with videos). *Gastrointest. Endosc.* **83**, 337–346 (2016).
5. Hashimoto, R. *et al.* Usefulness of the S-O clip for gastric endoscopic submucosal dissection (with video). *Surg. Endosc.* **32**, 908–914 (2018).
6. Ritsuno, H. *et al.* Prospective clinical trial of traction device-assisted endoscopic submucosal dissection of large superficial colorectal tumors using the S-O clip. *Surg. Endosc.* **28**, 3143–3149 (2014).
7. Matsuzaki, I. *et al.* Magnetic anchor-guided endoscopic submucosal dissection for gastric lesions (with video). *Gastrointest. Endosc.* **87**, 1576–1580 (2018).
8. Dobashi, A. *et al.* An internal magnet traction device reduces procedure time for endoscopic submucosal dissection by expert and non-expert endoscopists: Ex vivo study in a porcine colorectal model (with video). *Surg. Endosc.* **33**, 2696–2703 (2019).
9. Teoh, A. Y. *et al.* Ex vivo comparative study using the Endolifter(R) as a traction device for enhancing submucosal visualization during endoscopic submucosal dissection. *Surg. Endosc.* **27**, 1422–1427 (2013).
10. Ji, R. *et al.* Simplified robot-assisted endoscopic submucosal dissection for esophageal and gastric lesions: A randomized controlled porcine study (with videos). *Gastrointest. Endosc.* **96**, 140–147 (2022).
11. Kim, S. H. *et al.* Endoscopic submucosal dissection using a detachable assistant robot: A comparative in vivo feasibility study (with video). *Surg. Endosc.* **35**, 5836–5841 (2021).
12. Hwang, M., Lee, S. W., Park, K. C., Sul, H. J. & Kwon, D. S. Evaluation of a robotic arm-assisted endoscope to facilitate endoscopic submucosal dissection (with video). *Gastrointest. Endosc.* **91**, 699–706 (2020).
13. Fothergill, L. J. *et al.* Distribution and co-expression patterns of specific cell markers of enteroendocrine cells in pig gastric epithelium. *Cell Tissue Res.* **378**, 457–469 (2019).
14. Horii, J. *et al.* Which part of a porcine stomach is suitable as an animal training model for gastric endoscopic submucosal dissection?. *Endoscopy.* **48**, 188–193 (2016).
15. Chung, I. K. *et al.* Therapeutic outcomes in 1000 cases of endoscopic submucosal dissection for early gastric neoplasms: Korean ESD Study Group multicenter study. *Gastrointest. Endosc.* **69**, 1228–1235 (2009).
16. Probst, A., Maerkl, B., Bittinger, M. & Messmann, H. Gastric ischemia following endoscopic submucosal dissection of early gastric cancer. *Gastric Cancer* **13**, 58–61 (2010).
17. Kim, H. H., Park, M. I., Park, S. J. & Moon, W. Myocardial infarction thought to be provoked by local epinephrine injection during endoscopic submucosal dissection. *J. Clin. Med. Res.* **3**, 143–146 (2011).
18. Yang, X. *et al.* Novel miniature transendoscopic telerobotic system for endoscopic submucosal dissection (with videos). *Gastrointest. Endosc.* **99**(2), 155-165.e4 (2024).
19. Yang, X. X. *et al.* A novel flexible auxiliary single-arm transluminal endoscopic robot facilitates endoscopic submucosal dissection of gastric lesions (with video). *Surg Endosc.* **36**(7), 5510–5517 (2022).
20. Alfonso Forero Piñeros, E., Arantes, V. & Toyonaga, T. Endoscopic submucosal dissection (ESD) for early gastric cancer: State of the art. *Rev. Colomb. Gastroenterol.* **27**, 194–214 (2012).
21. Yang, X. *et al.* Robot-assisted endoscopic submucosal dissection contributes to efficient and safe learning for novices: Prospective pilot cross-over ex vivo study (with video). *Dig. Endosc.* **35**(3), 342–351 (2023).
22. Marin-Gabriel, J. C. *et al.* Use of electrosurgical units in the endoscopic resection of gastrointestinal tumors. *Gastroenterol. Hepatol.* **42**, 512–523 (2019).
23. Kim, B. G. *et al.* A pilot study of endoscopic submucosal dissection using an endoscopic assistive robot in a porcine stomach model. *Gut Liver* **13**, 402–408 (2019).
24. Chiu, P. W. Y., Ho, K. Y. & Phee, S. J. Colonic endoscopic submucosal dissection using a novel robotic system (with video). *Gastrointest. Endosc.* **93**, 1172–1177 (2021).
25. Mascagni, P. *et al.* Democratizing endoscopic submucosal dissection: Single-operator fully robotic colorectal endoscopic submucosal dissection in a pig model. *Gastroenterology* **156**, 1569-1571.e1562 (2019).
26. Hwang, M. & Kwon, D. S. K-FLEX: A flexible robotic platform for scar-free endoscopic surgery. *Int. J. Med. Robot.* **16**, e2078 (2020).
27. Carmichael, H., D'Andrea, A. P., Skancke, M., Obias, V. & Sylla, P. Feasibility of transanal total mesorectal excision (taTME) using the Medrobotics Flex(R) System. *Surg. Endosc.* **34**, 485–491 (2020).

28. Okamoto, Y. *et al.* Colorectal endoscopic submucosal dissection using novel articulating devices: A comparative study in a live porcine model. *Surg. Endosc.* **33**, 651–657 (2019).
29. Atallah, S., Sanchez, A., Bianchi, E. & Larach, S. W. Envisioning the future of colorectal surgery: Preclinical assessment and detailed description of an endoluminal robotic system (ColubrisMX ELS). *Tech. Coloproctol.* **25**, 1199–1207 (2021).

Acknowledgements
This work was supported by the National Research Foundation of Korea(NRF) grant funded by the Korean government(Ministry of Science and ICT) (No. 2019R1F1A1061414).

Author contributions
Joonhwan Kim: conception and design, analysis and interpretation of the data, drafting of the article. Dong-Ho Lee: analysis and interpretation of the data, drafting of the article. Dong-Soo Kwon: critical revision of the article for important intellectual content. Ki Cheol Park: process the excised tissue for pathological examination. Hae Joung Sul: conduct pathological examination. Interpretation of pathology result. Minho Hwang: development of the endoscope-attachable robot arm used in the study. Seung-Woo Lee: conception and design, perform animal experiments. Drafting of the article, final approval of the article.

Competing interests
Joonhwan Kim, Dong-Ho Lee, and Dong-Soo Kwon have stock ownership of Roen Surgical, Inc. Minho Hwang and Seung-Woo Lee hold a position on the advisory board of Roen Surgical, Inc. Hae Joung Sul and Ki Cheol Park have no conflict of interest.

Additional information
Supplementary Information The online version contains supplementary material available at https://doi.org/10.1038/s41598-024-63647-y.

Correspondence and requests for materials should be addressed to S.-W.L.

Reprints and permissions information is available at www.nature.com/reprints.

Publisher's note Springer Nature remains neutral with regard to jurisdictional claims in published maps and institutional affiliations.